Electronic Supporting Information (ESI)

Ferrite-based Soft and Hard Magnetic Structures by Extrusion Free Forming

*Erwin Peng[1], Xiangxia Wei[1], Tun Seng Herng[1], Ulf Garbe[2], Dehong Yu[2] and Ding Jun*[1]*

[1]Department of Materials Science and Engineering, Faculty of Engineering, National University

of Singapore (NUS), 7 Engineering Drive 1, Singapore 117574.

[2]*Australian Nucl Sci & Technol Org, Bragg Inst, New Illawarra Rd, Lucas Heights, NSW 2234,*

Australia

*Email: msedingj@nus.edu.sg

S1. Shear Rate Calculation During Extrusion
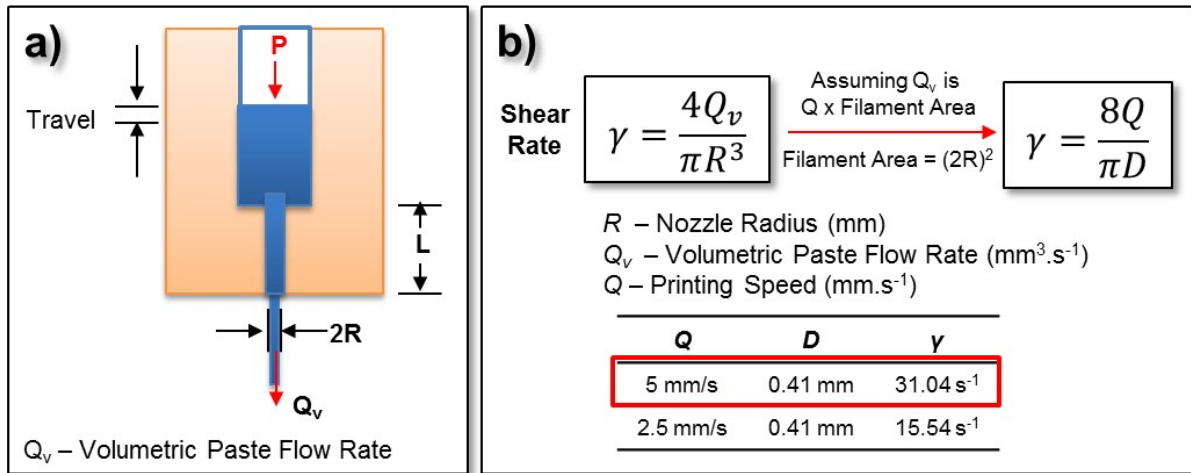
Fig. S1 Schematic diagram showing the extrusion process and its related shear rate calculation.

The extrusion free-forming process is illustrated in **Fig. S1a**. From this illustration, the ceramic paste loaded inside plastic syringe is driven by external pressure (P) through a small orifice (radius R; mm) at certain volumetric flow-rate (Q_v; mm^3.s^{-1}). Based on such configuration, the shear rate (γ) during the extrusion of the ceramic paste through small orifice can be calculated by using the equation given in **Fig. S1b** [1,2]. Several variables can be obtained from the printing settings. These include (i) the nozzle movement speed of 5 mm.s^{-1}, (ii) the nozzle diameter of 410 µm, and (iii) the layer thickness of 600 µm. By assuming the volumetric paste flow rate to be printing speed times the deposited filament cross sectional area (2R)^2, the calculated shear rate during the printing was approximated to be ~31.0 s^{-1}. It is essential to tailor the paste viscosity at desired shear rate to ensure the printability of the metal oxide paste.

S2. Low Magnification SEM Images of NiFe$_2$O$_4$ and BaFe$_{12}$O$_{19}$ structures
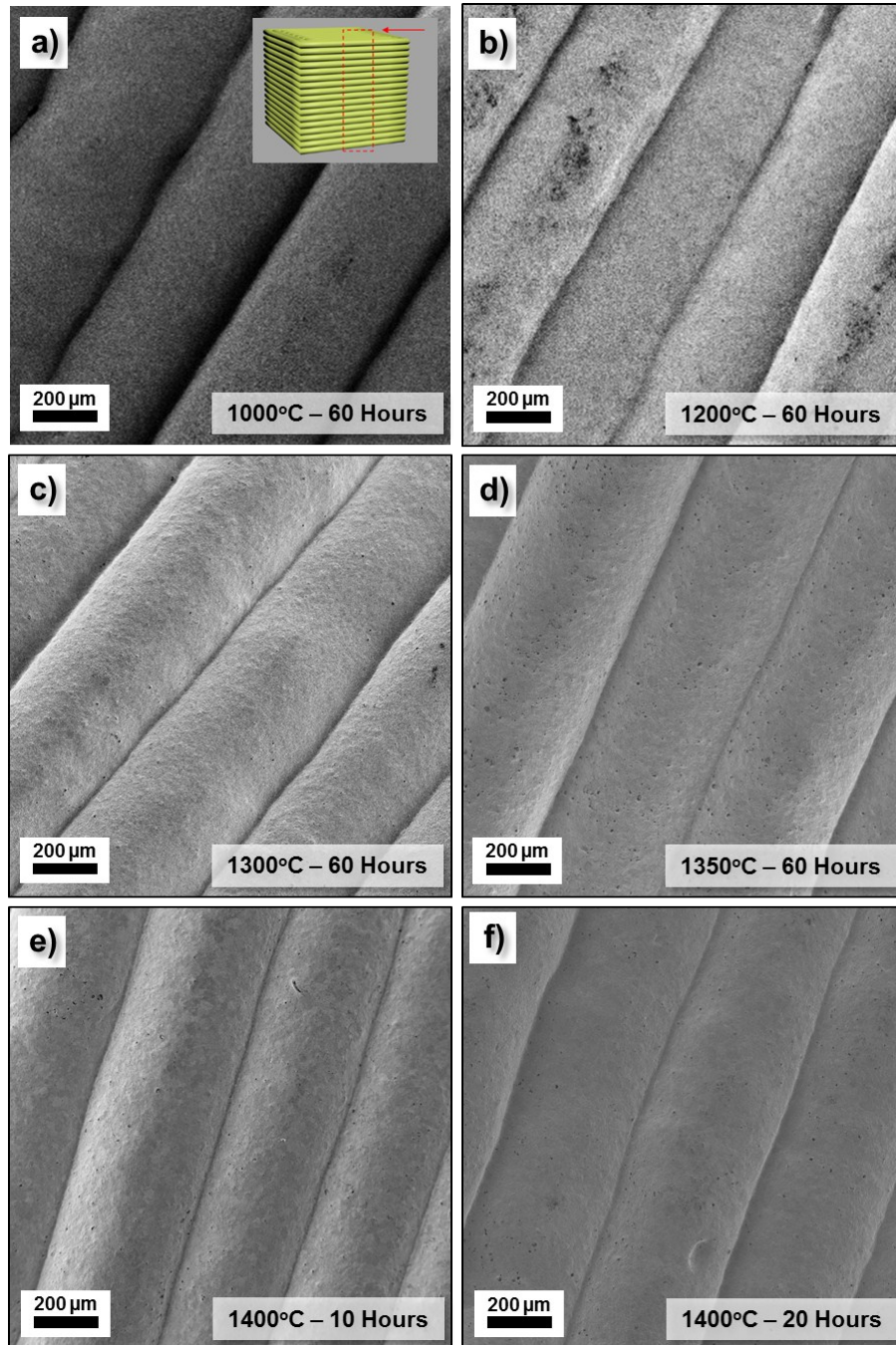
**Fig. S2** SEM images showing the microstructures of the sintered NiFe$_2$O$_4$ 3D printed structures at low magnification: (a) 1000°C/60Hours, (b) 1200°C/60Hours, (c) 1300°C/60Hours, (d) 1350°C/60Hours, (e) 1400°C/10Hours and (f) 1400°C/20Hours. The images showed the overview of the 3D printed filaments in the longitudinal direction.

As mentioned in section S1, the layer thickness (z-direction) setting was fixed at 600 μm for the printing process. Therefore, the green bodies of the printed $NiO.Fe_2O_3$ and $BaCO_3.Fe_2O_3$ structures were expected to have 600 μm thick layers. From the low magnification SEM images (**Fig. S2**) of bulk $NiFe_2O_4$ samples sintered at various conditions, the overview of the 3D printed filaments stacking in the longitudinal direction was revealed. In general, the deposited layers were around 400 – 500 μm in thickness. Such decrease in the layers thickness was attributed to the shrinkage in the z-direction by 25 to 30% during densification (elimination of solvent and organic additives). Similar trend was also observed for the bulk $BaFe_{12}O_{19}$ samples sintered at various conditions (as shown in the **Fig. S3**).
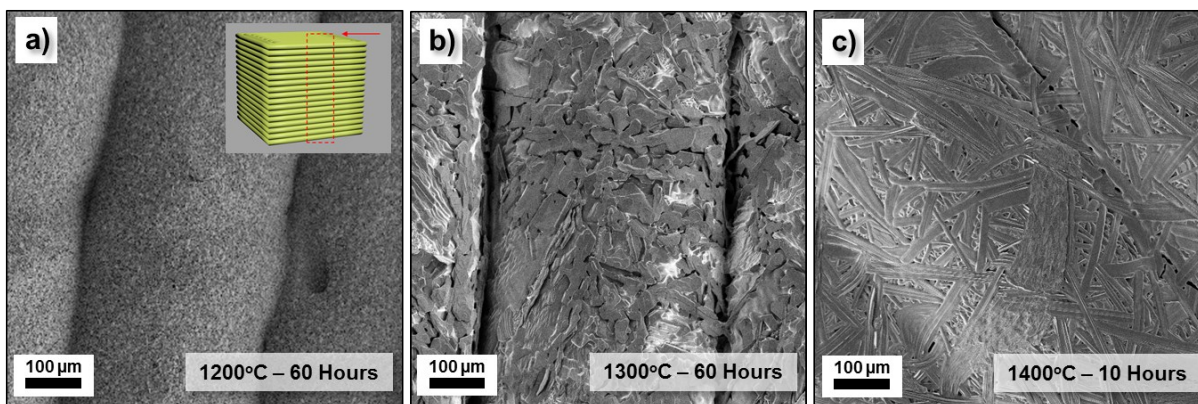
Fig. S3 SEM images showing the microstructures of the sintered $BaFe_{12}O_{19}$ 3D printed structures at low magnification: (a) 1200°C/60Hours, (b) 1300°C/60Hours and (c) 1400°C/10Hours. The images showed the overview of the 3D printed filaments in the longitudinal direction.

S3. EDX Spectrum of NiFe$_2$O$_4$ and BaFe$_{12}$O$_{19}$ Samples
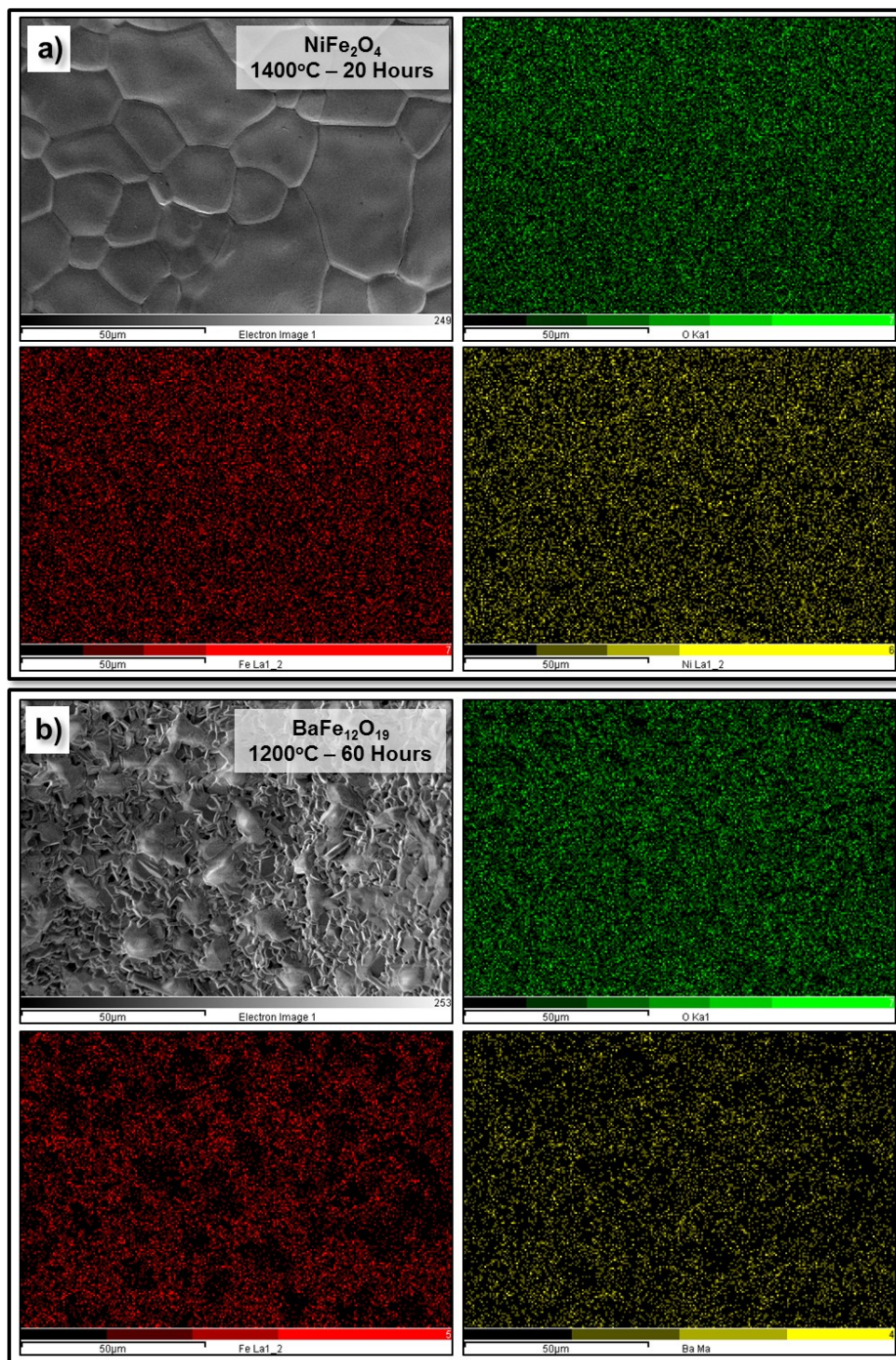

Fig. S4 SEM EDX elemental mapping of the bulk (a) NiFe$_2$O$_4$ and (b) BaFe$_{12}$O$_{19}$ 3D printed structure sintered at 1400°C/20Hours and 1200°C/60Hours respectively.

The EDX elemental mapping analysis of the bulk $NiFe_2O_4$ (1400°C/20 Hours) and $BaFe_{12}O_{19}$ (1200°C/60 Hours) surface were summarized in **Fig. S4**. The SEM image of $NiFe_2O_4$ (1400°C/20 Hours) suggested a dense polycrystalline structure without the presence of any residual porosity. Thus, the elemental mapping analysis in **Fig. S4a** indicated uniform distribution of Fe, Ni and O elements. On the other hand, as suggested from the SEM image of the $BaFe_{12}O_{19}$ (1200°C/60 Hours) surface, residual porosity were still presence in the sintered structures. Thus, the elemental mapping analysis in **Fig. S4b** clearly indicated the presence of such pores through the discontinuous distributions of Ba and Fe elements. The overall quantitative elemental compositions analysis of the $NiFe_2O_4$ and $BaFe_{12}O_{19}$ structures sintered at 1400°C/20Hours and 1200°C/60Hours were given in **Table. S1** below.

Table S1. Quantitative elemental compositions of $NiFe_2O_4$ and $BaFe_{12}O_{19}$ structures sintered at 1400°C/20Hours and 1200°C/60Hours.

Element	Weight %	Atomic %	Element	Weight %	Atomic %
Ni L	26.95	16.19	Ba L	34.58	64.05
Fe L	49.10	31.01	Fe L	2.93	2.80
O K	23.95	52.80	O K	62.49	33.15

S4. XPS Spectra of NiFe₂O₄ and BaFe₁₂O₁₉ structures
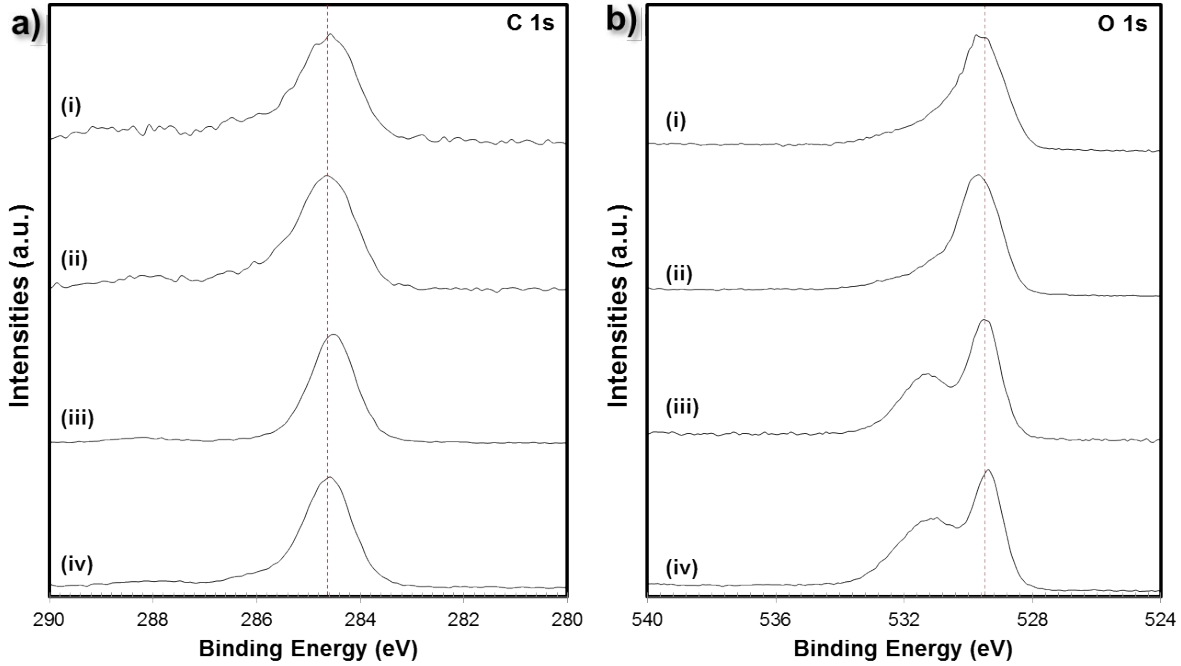
Fig. S5 XPS spectra of (a) C 1s and (b) O 1s for various 3D printed NiFe$_2$O$_4$ and BaFe$_{12}$O$_{19}$ samples: (i) BaFe$_{12}$O$_{19}$ (1200°C/60 Hours), (ii) BaFe$_{12}$O$_{19}$ (1300°C/60 Hours), (iii) NiFe$_2$O$_4$ (1350°C/60 Hours) and (iv) NiFe$_2$O$_4$ (1400°C/20 Hours).

The XPS C 1s and O 1s spectra of several of 3D printed NiFe$_2$O$_4$ and BaFe$_{12}$O$_{19}$ samples were summarized in **Fig. S5**. The C 1s peaks for all 4 samples were due to the small amount of carbon contamination from the ambient exposure of the samples. Meanwhile, the O 1s peaks for all 4 samples were observed at 529.4 eV for NiFe$_2$O$_4$ samples and 529.6 eV for BaFe12O19 samples which corresponds to O^{2-} anions of the pure composites. For NiFe$_2$O$_4$, a distinct characteristic peak at 531.3 eV of the O 1s peak was also observed. Such peak can be attributed to O^{2-} ions in the oxygen-deficient regions (*i.e.* O vacancies). This result suggested the presence of oxygen defects in the sintered NiFe$_2$O$_4$ surface. [3]

S5. Magnetic Properties Summary

Table S2. Summary of the magnetic properties of the sintered bulk $NiFe_2O_4$ and $BaFe_{12}O_{19}$ 3D printed structures

Sample	Sintering Conditions	M_S (emu.g^{-1})
$NiFe_2O_4$	1000°C – 60 Hours	38.32
$NiFe_2O_4$	1300°C – 60 Hours	46.44
$NiFe_2O_4$	1350°C – 60 Hours	48.39
$NiFe_2O_4$	1400°C – 20 Hours	42.24
$BaFe_{12}O_{19}$	1200°C – 60 Hours	64.94
$BaFe_{12}O_{19}$	1300°C – 60 Hours	60.63
$BaFe_{12}O_{19}$	1400°C – 10 Hours	63.03

S6. Shrinkage of 3D Printed Structure - Dimensions Measurement
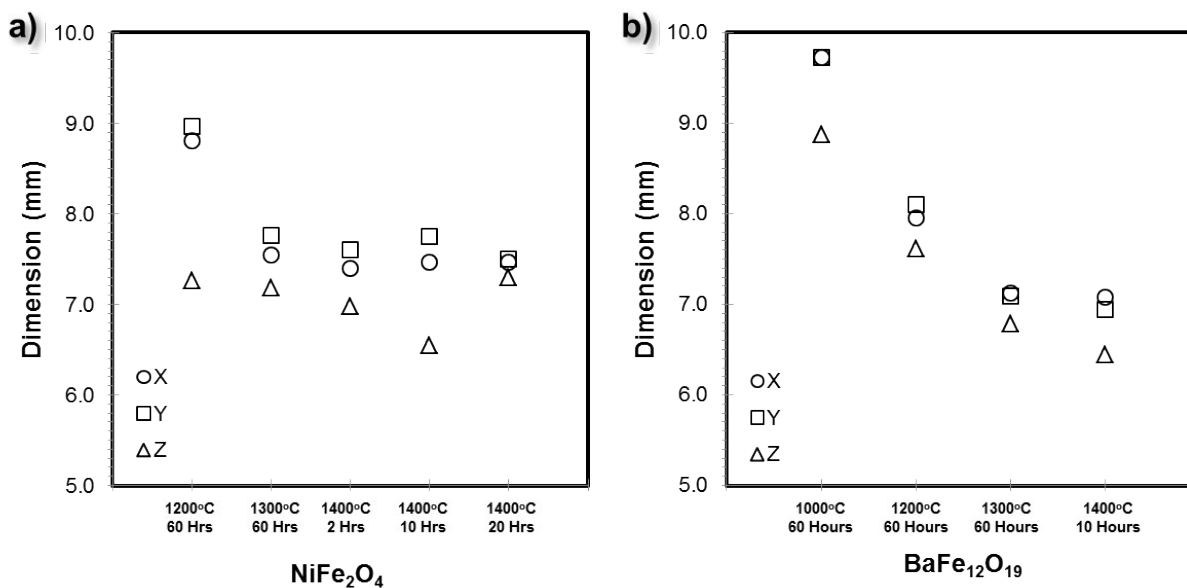
Fig. S6 Plot of the sintered 3D printed cubic structure dimensions against the sintering conditions: (a) $NiFe_2O_4$ and (b) $BaFe_{12}O_{19}$.

The volume shrinkage of the sintered 3D printed structure from its original green body dimensions were attributed to the evaporation of the solvent and the burn out of organic additives as well as pores elimination during densification process. During this process, the sample shrank

in all its three dimension (x,y,z). From **Fig. S6** and **Table S3**, the dimensional shrinkage of the 3D printed structure was more prominent in the longitudinal direction (z-axis) as compared to the lateral directions (x- and y-axis) suggesting the occurrence of non-uniform shrinkage.

Table S3. Summary of the sintered bulk $NiFe_2O_4$ and $BaFe_{12}O_{19}$ 3D printed structures density

Sample	Sintering Conditions	X (mm)	Y (mm)	Z (mm)	Density (g.cm^{-3})	Relative Theoretical Density
$BaFe_{12}O_{19}$	1000°C – 60 Hours	9.73	9.73	8.87	2.929	54.25%
$BaFe_{12}O_{19}$	1200°C – 60 Hours	7.95	8.10	7.61	4.137	76.61%
$BaFe_{12}O_{19}$	1300°C – 60 Hours	7.13	7.09	6.78	4.987	92.36%
$BaFe_{12}O_{19}$	1400°C – 10 Hours	7.08	6.94	6.44	5.063	93.76%
$NiFe_2O_4$	1200°C – 60 Hours	8.81	8.96	7.26	3.983	74.03%
$NiFe_2O_4$	1300°C – 60 Hours	7.54	7.76	7.18	4.984	92.65%
$NiFe_2O_4$	1400°C – 2 Hours	7.40	7.60	6.98	4.407	81.92%
$NiFe_2O_4$	1400°C – 10 Hours	7.47	7.75	6.54	4.783	88.91%
$NiFe_2O_4$	1400°C – 20 Hours	7.47	7.50	7.30	4.873	90.57%

Bulk Density of $BaFe_{12}O_{19}$: 5.40 g.cm^{-3}
Bulk Density of $NiFe_2O_4$: 5.38 g.cm^{-3}

S7. Neutron Radiography

The neutron imaging measurements were carried out at the neutron radiography instrument DINGO [4,5] at the OPAL research reactor (Sydney, Australia). The instrument is fed by a thermal neutron beam. The high resolution (16 μm) configuration is used in this experiment with neutron flux of 5.33 * 107 n/(cm^{2}s).

The sample stage, designed for heavy load, can be adjusted over 4 degrees of freedom (three translations and the rotary stage for tomography). The rotation stage has a positioning accuracy of 0.001°. The detector system comprises a scintillation screen, a mirror and a CCD camera. The camera is mounted at 90° from the beam direction; a mirror mounted at 45° is used to reflect the emitted light from the scintillation screen to the CCD. The scintillation screen used for this experiment is made of a 100 x 100 mm^2 aluminium sheet with 20μm thick layer of gadolinium-

oxide. The CCD camera (Andor IKON-L) is mounted on a translation stage to adjust the field of view to the experimental conditions of 15µm pixel size.

The tomography scans were run with 901 projections over 180º, with a step size of 0.2º and an exposure time of 6 x 20s. A set 6 images per projection was used to correct for "white spots" caused by gamma radiation. After correction we summed the 6 images to proceeds with the reconstruction process with the "Octopus" software package [6]. Sets of reference images of the empty beam for flat-field correction and background images (with closed shutter) have been taken as well. The total data acquisition time was about 45 hours including positioning time. The 3D rendering and visualisation including sectioning was done with the software package VGStudio by Volume Graphics [7].

Reference

1. J. Powell, S. Assabumrungrat and S. Blackburn, *Powder Technology*, 2013, 245, 21-27.

2. M. Faes, H. Valkenaers, F. Vogeler, J. Vleugels and E. Ferraris, *Procedia CIRP*, 2015, 28, 76-81.

3. Z. Shi, J. Zhang, D. Gao, Z. Zhu, Z. Yang, Z. Zhang and D. Xue, *Nanoscale Research Letters*, 2013, 8, 404.

4. Garbe, U; Randall, T; Hughes, C, The new neutron radiography / tomography / imaging station DINGO at OPAL, Nucl. Instrum. Methods Phys. Res., Sect. A 651(1), 42-46 (2011)

5. Garbe, U; Randall, T; Hughes, C; Davidson, G; Pangelis, S and Kennedy, SJ, A New Neutron Radiography / Tomography / Imaging Station DINGO at OPAL, Physics Procedia 69, 27-32 (2015)

6. M. Dierick, B. Masschaele & L. Van Hoorebeke, Measurement Science & Technology 15:7 (2004)

7. Volume Graphics, 2014. VGStudio MAX. URL: http://www.volumegraphics.com/en/